

Design study of a heavy ion fusion driver, HIBLIC†

**By T. KATAYAMA, A. ITANO, A. NODA,
M. TAKANAKA, S. YAMADA AND Y. HIRAO**

Institute for Nuclear Study, University of Tokyo, Tanashi, Tokyo 188, Japan

(Received 23 July 1984)

A heavy ion fusion (HIF) system, named HIBLIC (Heavy Ion Beam and Lithium Curtain) is conceptually designed. The driver system consists of RF linacs (RFQ linacs, IH linacs and Alvarez linacs), storage rings (one accumulator ring and three buncher rings) and beam transport lines with induction beam compressors. This accelerator complex provides 6 beams of 15 GeV²⁰⁸Pb¹⁺ ions to be focused simultaneously on a target. Each beam carries 1.78 kA current with 25 ns pulse duration, i.e., the total incident energy on the target is 4 MJ, 160 TW per shot. Superconducting coils are used in most parts of the magnet system to reduce power consumption.

1. General description of the driver

Beam parameters for the production of fusion energy are largely dependent upon the structure of the pellet containing the deuterium/tritium fuel. In the HIBLIC conceptual design, the target is designed as a cryogenic hollow shell of three concentric layers of lead, aluminium and fuel. It was shown (Niu 1984) that a relatively large target ($r_t = 4$ mm), imploded with 15 GeV Pb ions of 4 MJ, could produce a thermal output energy of 400 MJ. The peak power is 160 TW and the peak current and the total number of particles at the target are 10.7 kA and 1.7×10^{15} per shot, respectively. In table 1 the beam parameters from the target design are tabulated.

The number of beam lines is determined from two points of view. A uniform irradiation of the target surface is required to attain a high gain pellet design; hence a large number of beam lines is preferable. On the other hand, a simpler reactor design and beam transport system is possible for a small number of beam lines. Taking account of the beam transport capabilities per channel, the number of beam lines is optimized to be six.

The particle momentum spread at the final focus element has to be $\leq \pm 1\%$, otherwise the full beam cannot hit the target due to the chromatic aberration of the lenses, i.e. a large fraction of the beam misses the target. This constraint implies a momentum spread at the linac output of $\pm 7 \times 10^{-5}$ which imposes careful designs on the linac itself and the debuncher system. The admissible transverse emittance is determined by the considerations on the chromatic aberrations of the final focusing elements, space charge repulsive forces in the reactor and the stand off distance D from the target to the final focusing elements. For a beam radius of 3.2 mm and a D of 5.5 m, the emittance should not be larger than 80π mm mrad.

Within the limit of present RF linac technology it is impossible to accelerate a high current of 10.7 kA beams and then the provision of some current multiplication is

† From guest editors Y. Hirao and C. Yamanaka (Heavy Ion Beam Fusion Conference, Tokyo 23–27 Jan 1984).

| | |
|---------------------|------------------------|
| Ion species | $^{208}\text{Pb}^{1+}$ |
| Total beam energy | 4 MJ |
| Beam power | 160 TW |
| Pulse duration | 25 ns |
| Total beam current | 10.7 kA |
| Ion kinetic energy | 15 GeV |
| Number of beams | 6 |
| Radius of beam spot | 3.2 mm |
| Repetition rate | 10 Hz |
| Beam emittance | 80 π mm mrad |
| Momentum spread | ± 0.01 |

TABLE 1. Beam parameters.

necessary after the beam acceleration in the linac. In the present concept buncher rings are used for the current gain.

With I_L the peak current of the linac, S the stacking number in the ring, N_c the bunch compression factor and N_b the number of beam lines, the peak current I on the pellet is given by,

$$I = I_L \cdot S \cdot N_c \cdot N_b. \quad (1)$$

The bunch compression factor is 14 in the ring and 10 in the beam transport line, and therefore the total bunch compression factor N_c is 140, while the number of beam lines N_b is 6. In order to obtain the current of 10.7 kA on the pellet, $I_L \cdot S$ should be 12.7 A. If we stack the beam for five turns, both in the horizontal and vertical directions in the buncher ring, S is 25 and the linac current I_L is 510 mA, which would be attainable with the RF linac system.

When five turn injection into the betatron phase space is performed, blow up of the beam emittance is expected due to the space charge tune depression and the multiturn injection method itself. The dilution factor is simulated to be 2.67 and the transverse emittance of the linac beam ϵ_L should be smaller than 6.0 mm mrad (unnormalized) and 2.46 mm mrad (normalized), respectively.

The physical bunch length l_b at the pellet is $\beta c \tau$ where β is v/c and τ the pulse duration. In the present case, $\beta = 0.3722$ and $\tau = 25$ ns, and $l_b = 2.79$ m. As the total bunch compression factor is 140, the bunch length in the ring before the compression, should be $140l_b = 390.6$ m, and the ring circumference should be 781.7 m, as the harmonic number is two.

The maximum magnetic field strength of the superconducting dipole magnet in the ring is assumed as 5 Tesla and the radius of curvature ρ is given by,

$$\rho(m) = \frac{10p(\text{GeV}/c)}{3qB(\text{T})}, \quad (2)$$

where p is the momentum of the ions of charge state q . In the present case, p is 79 GeV/c for a kinetic energy of 15 GeV, and the relation of average radius R and ρ is nearly $R \approx 2.4\rho$ and finally the parameters of the buncher ring are as in table 2.

The number of ions which can be stored in a ring is limited by various beam instabilities. Firstly, the incoherent space charge force of the beam itself disturbs the focusing field of the magnet system. The maximum number of ions n is given by,

$$n = \frac{2\pi \cdot \Delta\nu \cdot A}{Br_p} \frac{1}{q^2} \epsilon \beta^2 \gamma^3, \quad (3)$$

| | |
|-------------------------------|---------------------------|
| Radius of curvature | $\rho = 51.80$ m |
| Average radius | $R = 124.41$ m |
| Circumference | $C = 781.66$ m |
| Number of bunches in one ring | $h = 2$ |
| Strength of magnetic field | $B = 5$ Telsa |
| Number of ions in one ring | $N = 5.57 \times 10^{14}$ |

TABLE 2. Parameters of buncher ring.

where B is a bunching factor, r_p ($= (1/4\pi\epsilon_0)/(e^2/Mc^2)$) is a 'classical proton radius', A is the mass number, q is a charge state and ϵ is the unnormalized beam emittance. For the values of $B = 1$, $A = 208$, $q = 1$, $\epsilon = 80$ mm mrad, $\Delta\nu = 0.25$, n is calculated at 2.2×10^{15} particles. From this argument, the minimum number of buncher rings is one.

Secondly, coherent beam instabilities make the amplitude of collective ion motion grow larger. They have been extensively studied at the CERN ISR for a high energy proton beam, and if we scale the data to a low energy heavy ion beam, the growth rates of instability are $150 \mu\text{s}$ for the longitudinal motion and 12.4 ms for the transverse motion. Thus the longitudinal instability might place a severe limit on the number of ions in the ring.

An accumulator ring with a circumference of 5 times larger than that of the buncher ring is prepared to perform the five turn injection into the buncher ring. Ions are also injected into the accumulator ring from the linac with the five turn injection method and are extracted by the one turn, fast ejection method. The extracted beam is x - y rotated in the transport line and is injected in the buncher ring. Hence 25 turn beams can be injected in the x - y betatron phase spaces in the buncher rings.

The linear accelerator system is required to accelerate high intensity heavy ions up to 15 GeV (75 MeV/u). The high brightness and high energy resolution are also important requirements for the output beam.

In the low velocity region, the required current of more than 0.5 A is far above the limiting current due to space charge effects. The limiting current, however, depends strongly on the ion velocity, so the funneled tree system on linacs is proposed to avoid the difficulty.

In the present design, 0.58 A of Pb^+ ions are produced by 16 ion sources of 32 mA each, and preaccelerated by 16 Cockcroft-Walton accelerators of 1 MV. The singly charged Pb ions are then bunched and accelerated to 0.30 MeV/u by 16 RFQ linacs followed by 8 funneling sections. The resonant frequency of the RFQ linacs is chosen to be 12.5 MHz, and the output beam bunches emerge from the linacs with the same frequency. Since the next interdigital H-type linac tanks have the doubled resonant frequency of 25 MHz, each IH linac can accept a pair of RFQ beams without decreasing the longitudinal phase space density. The transverse emittance can be kept constant if a carefully designed funneling system is installed.

| | RFQ | IH | Alvarez |
|---------------------|-----------|-----------|------------|
| Input energy | 5 keV/u | 300 keV/u | 4.5 MeV/u |
| Output energy | 300 keV/u | 4.5 MeV/u | 75 MeV/u |
| Frequency (MHz) | 12.5 | 25, 50 | 100, 200 |
| Length (m) | 500 | 238, 741 | 2000, 7400 |
| Number | 16 | 8, 4 | 2, 1 |
| Output current (mA) | 35 | 65, 130 | 260, 520 |

TABLE 3. Parameters of linac system.

Similar funneling sections are introduced at the particle energies of 1.16, 4.51 and 17.8 MeV/u, and a pair of linac beams is combined into a single beam at each section. The final stage of the linac system has an Alvarez type accelerating structure with a resonant frequency of 200 MHz. Therefore, the macroscopic peak current can be increased by a factor of 16 when the rf buckets of the 200 MHz Alvarez linac are all filled. The parameters of the linac system are given in table 3.

2. Linac system

2.1. Emittance considerations

The normalized longitudinal emittance of the output beam is required to be less than $7.7 \pi \text{ mm mrad}$, corresponding to an energy resolution of less than 10^{-4} (half value) after the debuncher. This high resolution is far better than that achieved by conventional proton linacs. In the case of heavy ions, however, the separatrix height of the rf buckets is reduced by a factor $\sqrt{q/A}$, where q and A are the charge state and mass number of the heavy ions to be accelerated. In the present case, this factor is about 14 and such a high energy resolution is not an unreasonable value.

The longitudinal emittance growth is serious especially during the bunching process due to the strong space charge forces. In the present design, the longitudinal emittance growth during the bunching process is estimated at factor of about 30. Qualitatively, the emittance growth can be reduced by adopting the slow bunching which leads to the long linacs.

At the output end of the RFQ linacs, the normalized longitudinal emittance and the energy resolution are $2.3 \pi \text{ mm mrad}$ and $\pm 2.4 \times 10^{-3}$ for a phase spread of 70 degree.

The normalized value of the required transverse emittance is less than $2.5 \pi \text{ mm mrad}$ and about 5 times larger than the estimated emittance of the ion sources. The main sources of the transverse emittance growth are funneling process, space charge effects, misalignments of the Q-lenses in the drift tubes, etc. These effects must be kept to a minimum.

In table 4, the assumed values of emittances are given at each stage of the linac system.

| | Transverse ($\pi \text{ mm mrad}$) | Longitudinal ($\pi \text{ mm mrad}$) |
|-----------------------|---|---|
| After Preaccelerators | 0.50 | 0.083 |
| 12.5 MHz RFQ | 0.69 | 2.3 |
| 25 MHz IH | 0.95 | 3.1 |
| 50 MHz IH | 1.3 | 4.2 |
| 100 MHz Alvarez | 1.8 | 5.7 |
| 200 MHz Alvarez | 2.5 | 7.7 |

TABLE 4. Normalized longitudinal and transverse emittance at each stage of linac system.

2.2. Focusing with quadrupole magnets in the drift tubes

As focusing elements in the drift tubes, magnetic quadrupoles are preferable to electrostatic quadrupoles because of the high voltages required by quadrupole electrodes. The focusing sequence of FFFDDD is chosen in order to keep the poletip magnetic field below 10 kG. In conventional proton linacs, this focusing sequence is not adopted because the stable region of the betatron oscillations is quite narrow compared

| | IH 25 MHz | IH 50 MHz | Alvarez 100 MHz | Alvarez 200 MHz |
|--|--------------|--------------|--------------------|--------------------|
| Accelerating Field (MV/m) | 1.0 | 1.2 | 1.6 | 1.8 |
| Synchronous Phase (deg) | -43.6 | -41.1 | -33.5 | -30.7 |
| Focusing Strength | 0.5 | 0.25 | 0.14 | 0.07 |
| RF Defocusing Parameter ($\times 10^{-4}$) | -19~-9.6 | -5.3~-2.9 | -1.7~-0.87 | -0.38~-0.16 |
| Field Gradient (kG/cm) | 8.5~4.3 | 8.7~4.4 | 9.9~5.1 | 10.2~5.5 |
| Bore Radius of Q-magnets (cm) | 0.69~0.79 | 0.66~0.76 | 0.93~1.1 | 1.0~1.2 |
| Magnetic Flux at the Pole Tip (kG) | 5.9~3.4 | 5.7~3.3 | 9.2~5.5 | 10.6~6.6 |

TABLE 5. Specifications of quadrupole magnets in the drift tubes.
The focusing sequence is FFFDDD.

with the FD or FFDD sequences. For heavy ions, however, it is possible to keep the transverse acceptance stable due to the small value of the charge to mass ratio. The focusing strength is as small as 0.5 for the 25 MHz IH linac and 0.07 for the 200 MHz Alvarez. The bore radius of the Q-magnets varies from 0.7 cm for the 25 MHz IH to 1.2 cm for the 200 MHz Alvarez. More detailed parameters are given in table 5.

2.3. Funneling section

As already mentioned, the funneling sections combine a pair of low frequency beams into a single beam of higher frequency. Each beam bunch is captured into one rf-bucket. So, the macroscopic peak currents increase by a factor of 2 maintaining the longitudinal emittance constant.

The size of the beam bunches before and after the funneling process are not much different. The space charge forces in the bunch, therefore, will not be affected much.

In order to realize the funneling process, the high frequency deflector system must be installed. A rectangular waveform of the deflector voltage is the best to avoid transverse emittance growth. A sinusoidal waveform will also be acceptable if special care is taken to shape the longitudinal emittance. With sinusoidal deflection, sharp phase focusing is required at the deflector positions. Since the short beam bunches produce strong space charge forces, sinusoidal deflection necessarily brings about the emittance growth. In the present design, the low velocity funneling sections, where the space charge forces play the more important roles, are designed with a rectangular waveform. A summary of the important parameters of the funneling sections is given in table 6.

| | F1 | F2 | F3 | F4 |
|--|-------|------|------|-------|
| T (MeV/u) | 0.3 | 1.6 | 4.51 | 17.78 |
| $\beta\lambda/2$ (m) | 0.3 | 0.3 | 0.29 | 0.28 |
| Frequency (MHz) | 12.5 | 25 | 50 | 100 |
| Number of deflector | 9 | 9 | 9 | 12 |
| Deflector field [†] (MV/m) | 0.542 | 2.09 | 9.8 | 19.3 |
| Voltage [‡] (KV) | 22 | 84 | 390 | 770 |
| Buncher voltage (MV) | — | — | 5.3 | 10.6 |
| Length between buncher and deflector (m) | | | 176 | 34.7 |

TABLE 6. Parameter list of funneling sections.

[†] The gap between the deflector plates is assumed to be 4 cm.

[‡] The waveforms of the high voltage applied to the deflectors are rectangular for F1 and F2, and sinusoidal for F3 and F4.

3. Accumulator and buncher ring

3.1. Accumulator ring

In the design of the accumulator ring, the following conditions should be taken into account.

- (i) The circumference of the accumulator ring should be 5 times that of the buncher rings so as to perform 5 turn injection into the buncher ring.
- (ii) It is necessary to shorten the filling time of three buncher rings, because the growth rate of the longitudinal coherent instability in the buncher ring is as short as $150 \mu\text{s}$.

From the first condition, the circumference of the accumulator ring is found to be 3908.31 m . From the second condition, the three successive injections into the accumulator ring, to provide the beams for the three buncher rings, should be done as fast as possible. Considering the limited repetition rate of bump magnets for injection, three different injection systems would be necessary. Assuming three long straight sections for each injection system, nine straight sections are needed for injection. Similar problems due to the limited repetition rate are also anticipated for the kicker magnets for beam ejection from the accumulator ring, so that three different ejection systems are needed. Providing 2 long straight sections for each ejection system, a total 6 straight sections are required for ejection. Considering the above conditions, the superperiodicity is determined to be 16. So as to reduce the number of magnets and to make the focusing smooth, the cell length is chosen rather long (59 m) and the number of normal FODO cells are set to be 64. The average radius of the accumulator ring is five times larger than the buncher ring of the same magnetic rigidity of the beam, so a bending field of 1 T is sufficient. In order to facilitate 5 turn injection with large space charge tune depression, the betatron tune value is set around 12.25.

3.2. Buncher ring

The magnetic rigidity of a $^{208}\text{Pb}^{1+}$ beam with a kinetic energy of 15 GeV is 259.01 T m , so the radius of curvature becomes 51.80 m if a superconducting dipole strength of 5 T is assumed. The basic focusing structure is chosen to be $\text{F}\bar{\text{O}}\text{D}\bar{\text{O}}$ so as to make the drift spaces as long as possible within the same circumference. For the long straight sections, an $\text{F}\bar{\text{O}}\text{F}$ structure is used to make α ($= -1 d\bar{\beta}/2 ds$) zero at the position of the inflector septum, which seems to be essential to make a 5 turn injection without beam loss on the septum. From the point of view of providing enough space for RF cavities for bunch compression and equipment for injection and ejection, 8 long straight sections need to be made, so the superperiodicity of the ring becomes 8. It is desirable that the beam size should vary smoothly to reduce the defocusing effect due to space charge force. From this point of view, the cell length is chosen rather long and the betatron tune value is set to be relatively low, viz. 6.25 . In this design, drift spaces of total length 220 m are available, which seems adequate to attain the necessary bunch-compression voltage.

4. Multiturn injection into rings

The energy of the beam to be injected into a given ring amounts to 1.3 MJ for the present scenario, so the usual multiturn injection which involves beam collision with the inflector septum cannot be used, because the septum would melt away in a short time. In this section an injection scheme is described which attains a 5 fold increase of the peak current without beam loss, and within a limit of transverse beam emittance acceptable for the target and beam transport design. A beam emittance (unnormalized)

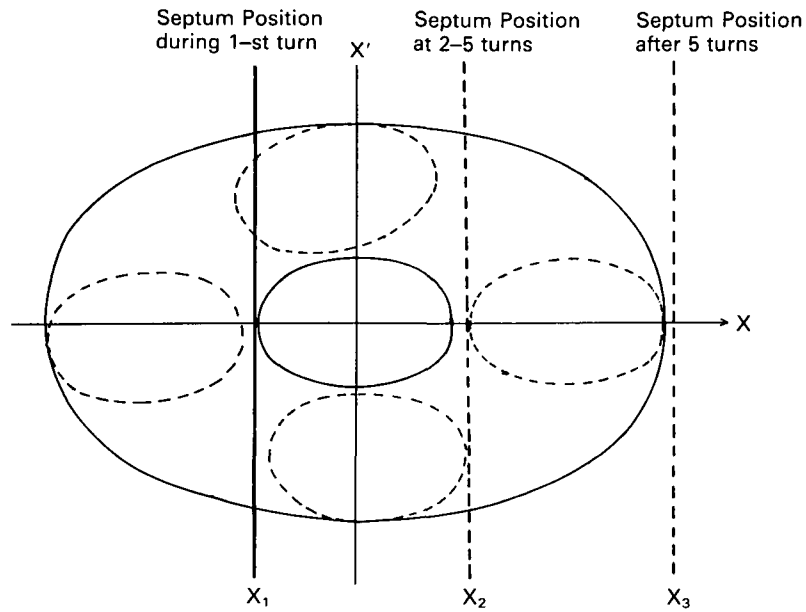


FIGURE 1. Acceptance ellipse in $x-x'$ phase space and injected beam shapes.

of $6 \pi \text{ mm mrad}$ is assumed and five turn injection into an acceptance of $80 \pi \text{ mm mrad}$ is discussed.

To perform five-turn injection under the condition of rather larger space charge tune depression, the following injection scheme is conceived.

(i) The beam is injected into the center of the acceptance ellipse in $x-x'$ phase space. At that time, the beam ellipse is matched to the acceptance shape (figure 1) by adjustment of magnet elements of the transport system. The orbit position with respect to the inflector septum is set at x_1 .

(ii) After 1 turn, the orbit position is shifted to x_2 and beam is injected into the outer shell of the acceptance ellipse during four turns.

(iii) After five turns, the inflector position is shifted outside the acceptance ellipse (x_3). It should be noted that the condition of α to be zero at the inflector position is indispensable in order to perform the above injection scheme without beam collision with the septum.

In this scheme, the dilution factor of transverse phase density is 2.67 for a five times peak current increase. Detailed numerical calculations of this injection scheme which take the space charge effect into account are described in the following section.

The results of the simulation of multiturn injection into the accumulator and the buncher rings are studied, using a two-dimensional program which takes account of the space charge effect.

Into the accumulator ring the $^{208}\text{Pb}^{+1}$ beam with a velocity of $\beta = 0.37$, an intensity of $I/\text{turn} = 0.51 \text{ A}$, and an emittance of $\epsilon_x = \epsilon_y = 6 \text{ mm mrad}$ is injected from the linac system. During the injection, the emittance parameters ($\alpha_i, \beta_i; i = x, y$) of the injected beam are kept fixed and the equilibrium orbit is shifted once.

SCOP2 is a two-dimensional simulation program (Bozsik *et al.* 1981) which has been developed to study space charge effects on an ion beam passing through on a

multiturn-injected beam in the ring. Each turn is assumed to be represented by a macrocanonical distribution simulated by 256 macro-particles.

As a lattice structure of the accumulator ring, a continuous focusing system is assumed to avoid too much CPU time. The acceptance at the injection point is $\alpha_x = \alpha_y = 0$ and $\beta_x = \beta_y = 50.8$ m for the accumulator ring and those of the buncher ring are $\alpha_x = \alpha_y = 0$, $\beta_x = 28.4$ m and $\beta_y = 13.2$ m, respectively.

Simulations are carried out by injecting beamlets without beam loss at the inflector septum of 2 mm thickness so that after 5 turns the beamlet of the first turn populates on the central region in the $x-x'$ plane and those of the other four turns circulate around the central region at intervals of about 90° . Additionally, the tune is adjusted so as to compensate the tune shift induced by the space charge effect.

On the first turn in the accumulator ring the space charge induces a Laslett-tune shift of 0.127 for $\nu = 12.25$.

On the successive beam injections, beamlets rotate in the phase plane by an angle of less than 90° due to the tune depression. Finally the beam distribution is given as in figure 2. When the tune value is shifted to 12.27, however, the beamlets of the four turns rotate just 90° on the $x-x'$ plane and the tune depression is compensated. The distortion of beam emittance becomes larger near the central region. The emittances ϵ_x

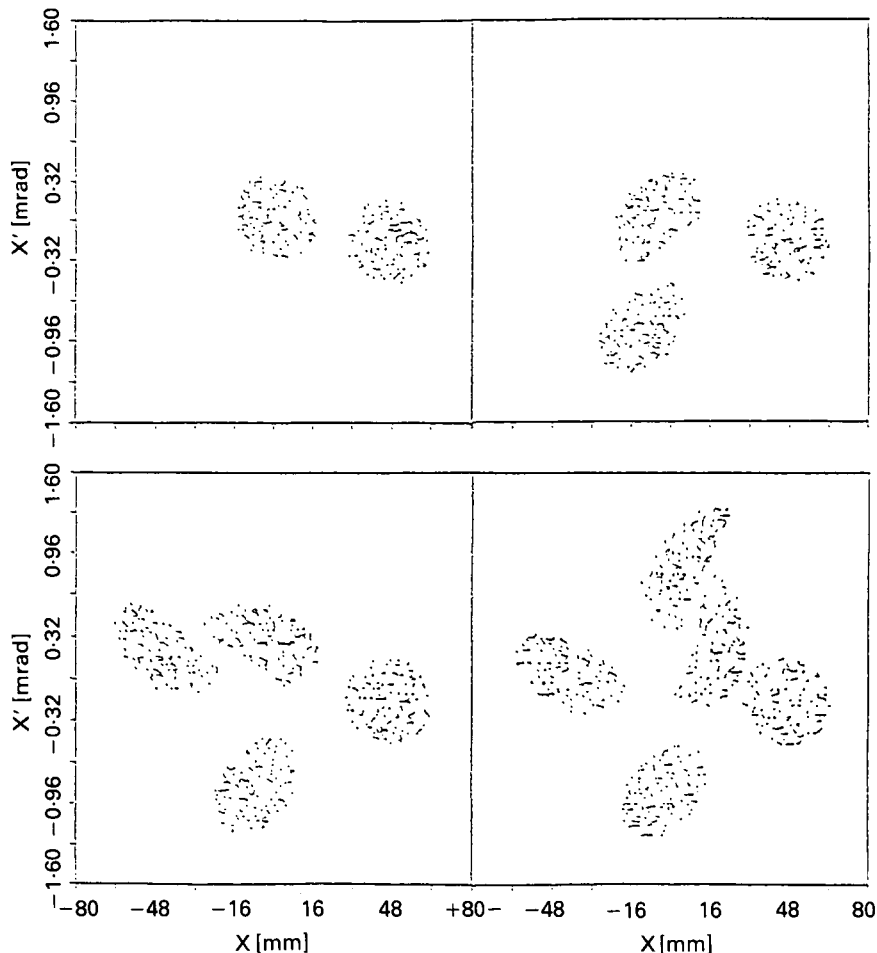


FIGURE 2. X-emittance during the injection of 5 turns into the accumulator ring.

and ε_y , after the injection of 5 turns are estimated 80 mm mrad and 6.6 mm mrad, respectively and there is no beam loss at the septum.

A Laslett-tune shift of 0.029 is found in the buncher ring for $\nu = 6.75$. The injection of 5 turns into the buncher ring suffers less from space charge effects than that in the accumulator ring. The horizontal emittance is increased from 6π mm mrad to 77π mm mrad during the multiturn process. When the fractional value of ν is 0.75, the central beamlets in the $x - x'$ plane get near the septum just after two turns due to the repulsive force from the beamlet of the second turn. When the fractional value is 0.25, the central beamlet goes away from the septum. Then even if initial horizontal emittance is 7.5π mm mrad, the injection of 5 turns is still possible with $\nu = 6.25$.

5. Beam instabilities in the buncher ring

In the present scenario, an accumulator ring and three buncher rings are to be used to achieve the required peak intensity on the target. In these rings various kinds of beam instabilities are anticipated which lead to emittance dilution in transverse and longitudinal phase spaces. In the buncher ring the current is 5 times higher than that in the accumulator ring and then the instability constraints are more severe. Here the results studied on the buncher ring are described.

5.1. Transverse coherent instability

The coasting beam stability limit for the transverse coherent wall instability is given as follows (Zotter, 1977),

$$I_0 \leq 4F \frac{AE_0 \nu \beta \gamma}{qe |Z| R} \left[|(n - \nu)\eta + \xi| \frac{\Delta p}{p} + \frac{\partial \nu}{\partial a^2} \Delta a^2 \right], \quad (4)$$

where I_0 , E_0 and Δp are the electric current of the beam, the rest mass of the proton and the full momentum spread at half height respectively and, Z represents the beam's transverse coupling impedance with an environment such as a vacuum chamber and can be written as,

$$Z = iRZ_0 \left[\frac{1}{\beta^2 \gamma^2} \left(\frac{1}{a^2} - \frac{1}{b^2} \right) - (1 + i) \frac{\delta}{b^3} \right]. \quad (5)$$

In the present case of the HIF buncher ring, real and imaginary parts of Z are 3.7×10^5 (Ω/m) and 1.7×10^8 (Ω/m), respectively. Assuming $\xi \left(\equiv \frac{\partial \nu}{\partial (\Delta p/p)} \right)$ to be -10 and no amplitude-dependent tune spread, the threshold current of this instability is calculated at 0.215 A, which corresponds to the circulating ion number of 9.4×10^{12} . Hence the threshold of this instability is more than 1 order lower than the number of ions to be accumulated in a buncher ring.

The e -folding growth time, τ is given by the relation,

$$\frac{1}{\tau} = \frac{cI_0 R_c(Z) qe}{4\pi \nu \gamma A E_0} \quad (6)$$

and is calculated at 12.4 ms, which is long enough compared with the time necessary for beam bunch compression in the buncher ring.

Summarizing the above discussion, the transverse resistive wall instability will occur, but should not be harmful until the bunch compression is completed and beam is extracted.

5.2. Longitudinal coherent instability

The threshold current of this instability is given by the Keil-Schnell criterion (Keil et al. 1969),

$$\left| \frac{Z_{11}}{n} \right| \leq F \frac{Am_0 c^2 \beta^2 \gamma |\eta| (\Delta p/p)^2}{qeI_0} \quad (7)$$

where Z_{11} is the longitudinal coupling impedance of the beam with an environment such as a vacuum chamber. For the ideal case of cylindrical beam and vacuum chamber, Z_{11} is given as follows,

$$\frac{Z_{11}}{n} = \frac{i}{2} \frac{Z_0}{\beta \gamma^2} \left[1 + 2 \ln \left(\frac{b}{a} \right) \right]. \quad (8)$$

Assuming the value of 2 for g ($= 1 + 2 \ln(b/a)$), $|Z_{11}/n|$ is calculated at $872.5 \text{ } (\Omega)$ and the threshold current is estimated at 1.114 (A) , which corresponds to ion number of 4.87×10^{13} . Thus also this instability is anticipated to occur.

From the dispersion relation,

$$(V' + iU')J = 1, \quad (9)$$

the stable region for this instability is calculated for a parabolic distribution as shown in

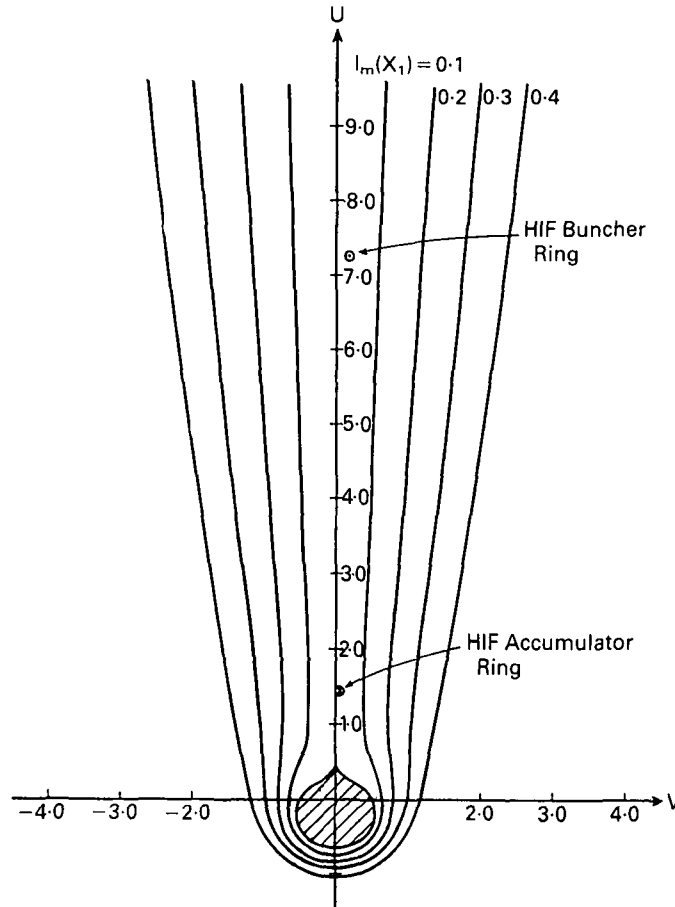


FIGURE 3. Stability diagram of longitudinal instabilities.

figure 3. From the relation,

$$V' + iU' = \frac{2I_0 e \cdot q}{Am_0 c^2 \beta^2 \gamma |\eta| (\Delta p/p)^2} \left(\frac{Z_r}{n} + \frac{Z_i}{n} \right), \quad (10)$$

where Z_r and Z_i denote real and imaginary parts of Z_{11} , respectively, V' and U' are calculated at 0.21 and 7.26, respectively if the value of 25Ω is assumed for Z_r/n (Möhl, 1979). In the figure this is indicated together with the case of the accumulator ring. It is known that both cases are far from the stable region. The $I_m(x_1)$ for the present case is read to be 0.036 and the maximum mode number of this instability is thought to be around 2500, so the growth rate τ is calculated by the relations,

$$\frac{1}{\tau} = nSI_m(x_1) \quad S = -\frac{1}{2}\eta\omega_0 \frac{\Delta p}{p}, \quad (11)$$

which leads to the result of $\tau \approx 150 \mu\text{s}$. This time is rather short compared with the necessary time for bunch compression. An experimental approach to reduce the real part of Z_{11} would be inevitable to manage this instability for the HIF buncher ring.

From the above discussion, it is found that only the longitudinal coherent instability in the buncher rings might cause a severe problem. However we have assumed the real part of the longitudinal coupling impedance to be 25Ω from the experience at CERN ISR. The growth rate largely depends on this value, so an experimental approach to reduce Z_r might be inevitable to manage this instability in connection with HIF driver design.

6. Beam bunching in the buncher ring

In this scenario, bunching by a factor of 14 is assumed in the buncher ring where two bunches, containing 2.8×10^{14} ions each, are made to rotate in $(\Delta p/p, \phi)$ space by applying a linear RF field. A linear rotation is necessary to prevent filamentation. Careful attention should be paid to both the space charge compensation and bunch rotation voltages, and the bunching time should at most be comparable to the blow up time of longitudinal microwave instabilities. Horizontal beam emittance growth due to the crossing of resonance lines during the bunching is a critical problem with the tight emittance limit of $80 \pi \text{mm mrad}$ imposed by the small beam spot on the target.

The space charge field per unit length in the ring is given by,

$$E_z = -\frac{gqe}{4\pi\epsilon_0\gamma^2} \frac{\partial\lambda}{\partial z} \quad (12)$$

where g is a geometrical factor $g = 1 + 2 \ln b/a - (r/a)^2$, and λ is the line density.

We assume a parabolic beam distribution,

$$\lambda(z) = \lambda_0 \left[1 - \left(\frac{2z}{l} \right)^2 \right] \quad (13)$$

where l is total bunch length. Substituting $\lambda(z)$ into (12) we get,

$$E_z = -\frac{3qgeN}{2\pi\epsilon_0\gamma^2 l^2} \quad (14)$$

at the bunch ends where the space charge field is maximum. The maximum voltage per turn in the ring is then $\pm 2\pi RE_z$ which can be rewritten as,

$$V = \frac{3Nqe}{2T^2} L \quad (15)$$

| | |
|---|--|
| Number of particles/bunch | 2.83×10^{14} |
| Initial bunch width | $= 1.72 \mu\text{s}$ |
| Final bunch width | $= 0.123 \mu\text{s}$ |
| Frequency of saw tooth wave | 300 KHz |
| Longitudinal space charge impedance | $-850.6 \text{ j}\Omega$ |
| Inductance | $9.28 \times 10^{-4} \text{ H}$ |
| Momentum spread | $= 1.14 \times 10^{-4} - 1.6 \times 10^{-3}$ |
| Compensation voltage for space charge force | $= 4.26 \text{ MV}$ |
| Bunch rotation voltage | $= 260 \text{ KV}$ |

TABLE 7. Compression in buncher ring.

where $2T$ is the bunch length in sec and L is space charge inductance,

$$L = \frac{gZ_0}{2\beta\gamma^2\omega_0} \quad (16)$$

with ω_0 = revolution angular frequency, and Z_0 = characteristic impedance of free space (120π ohms).

Initially, this longitudinal space charge force is small compared with the bunch rotation voltage, but the forces at the bunch ends drastically increase, inversely as the square of the bunch length. As shown in table 7, it needs up to 4.2 MV to compensate the repulsive space charge forces.

If the space charge force is continuously compensated by RF cavities in the ring, the number of revolutions to reach a peak value of the momentum spread $\Delta p/p$ at the quarter synchrotron oscillation point, n , is given by,

$$n = \pi/(4\eta h \Delta p/p) \quad (17)$$

and the RF voltage required to produce the bunch rotation is,

$$qeV = \pi^2\beta^2\gamma Am_0c^2/(8\eta hn^2) \quad (18)$$

where $\eta = |\gamma^{-2} - \gamma_i^{-2}| = 0.832$ is a dispersion of the ring, and A is the mass number. For 15 GeV Pb^{1+} ions, a linear RF focusing field of 270 KV is sufficient; n is 295 turns for the max $\Delta p/p$ of 1.6×10^{-3} . Bunching time nT is then 2.02 ms which might be too long considering the blow-up time of longitudinal microwave instabilities.

A ferrite loaded resonant cavity module can produce a low frequency 300 KHz RF field with an amplitude of 50 KV.

Using improved Mn-Zn ferrites with a permeability of $\sim 5000 \mu_0$, a one meter long module can be tuned to the desired frequency with an extra gap capacitance of 2000 pF. In the buncher ring 90 cavities are installed to produce the peak voltage of 4.5 MV and nearly the same number of cavities can be used to excite the higher harmonics so as to obtain the linearly rising field.

7. Beam transport, bunch compression and final focusing

Stable transport of intense heavy ion beams (1.8 kA per channel) from the accelerator to the fusion reactor chamber and focusing on a small target pellet are the most crucial problems in heavy ion fusion. The ballistic beam transport through long periodic transport lines in vacuum ($\leq 10^{-7}$ Torr) has been recognized to be more tractable than a plasma channel transport.

To obtain these high current beams, the beams extracted from the buncher rings are compressed longitudinally during their drift through the transport lines. The current limit transportable through the long periodic transport line is not so serious as long as a low charge state ion is chosen ($q = 1$). Space charge repulsion in the final focusing can be compensated by increasing the beam divergence, hence the radius of the entry port of the reactor. The lens apertures are limited by spherical aberrations. From the point of view of the chromatic aberrations, the transverse emittance and momentum spread should be as small as possible. A reasonable compromise between accelerators and final focus design has been found at around $80 \pi \text{mm mrad}$ transverse emittances and a 0.5–1.0% momentum spread.

Beam dynamic effects due to space charge play an important role in all of these processes; periodic transport, longitudinal bunch compression and final focusing. These subjects have been studied at the various HIF workshops. Here space charge aspects are recalled and numerical calculations for the HIBLIC scenario are presented.

7.1. Periodic transport and transverse stability

Beam transport from the buncher ring to the reactor chamber requires a length of 1 to 2 km to perform a longitudinal bunch compression. It is then necessary to ensure stable beam transport over a large number of periods of a quadrupole FODO focusing lattice without emittance growth. Space charge induced instabilities, i.e., emittance growth limits the transport current.

The mechanisms, through which a space charge field can cause emittance growth, are resonant coupling to the periodic structure, anisotropy between different degrees of freedom and a non-monotonic distribution function. Among these sources of space charge instabilities the first will be dominant in the present case.

For zero current, the requirement for stable transport is $\sigma_0 \leq 180^\circ$, where σ_0 is the phase advance per focusing period, to avoid a half-integer resonance with the focusing period. For finite current, the space charge force depresses the tune to a value $0 < \sigma < \sigma_0$, and coherent oscillation of the beam can be in resonance with the period of the focusing system.

Analytic theory (Smith *et al.*, 1977; Laslett *et al.* 1979) and computer simulations (Lapostolle 1978; Haber 1979; Haber *et al.* 1979; Penner *et al.* 1979) show that the quadrupole (i.e., envelope) modes of oscillation are stable if $\sigma_0 \leq 90^\circ$, whereas the sextupole (i.e., third-order) modes require $\sigma_0 \leq 60^\circ$ to avoid resonance. The higher order modes of oscillation have no effect on the r.m.s. emittance.

The considerations on coherent instabilities show the possibility of unlimited current transport through periodic channels with a zero intensity-phase advance $\sigma_0 = 60^\circ$ for beams with equal or almost equal horizontal and vertical emittances. Hence the practical limitation on current intensity is set by the design of the magnet lattice of the periodic transport channel.

By solving the scaled Kapchinskij-Vladimirskij envelope equations (Kapchinskij *et al.* 1959) we obtained the numerical results of the scaling laws for the case of a Pb^+ beam with a kinetic energy of 15 GeV and $\varepsilon = 8 \times 10^{-5} \text{ m rad}$ transported through an FODO lattice with $\sigma_0 = 60^\circ$ and $\eta = \frac{1}{2}$ (figure 4). The three curves correspond to different field strengths at the maximum envelope.

7.2. Longitudinal bunch compression in the final beam line

To obtain high current beams at the target in the fusion reactor, the ion beams extracted from the buncher ring are longitudinally compressed during the final beam

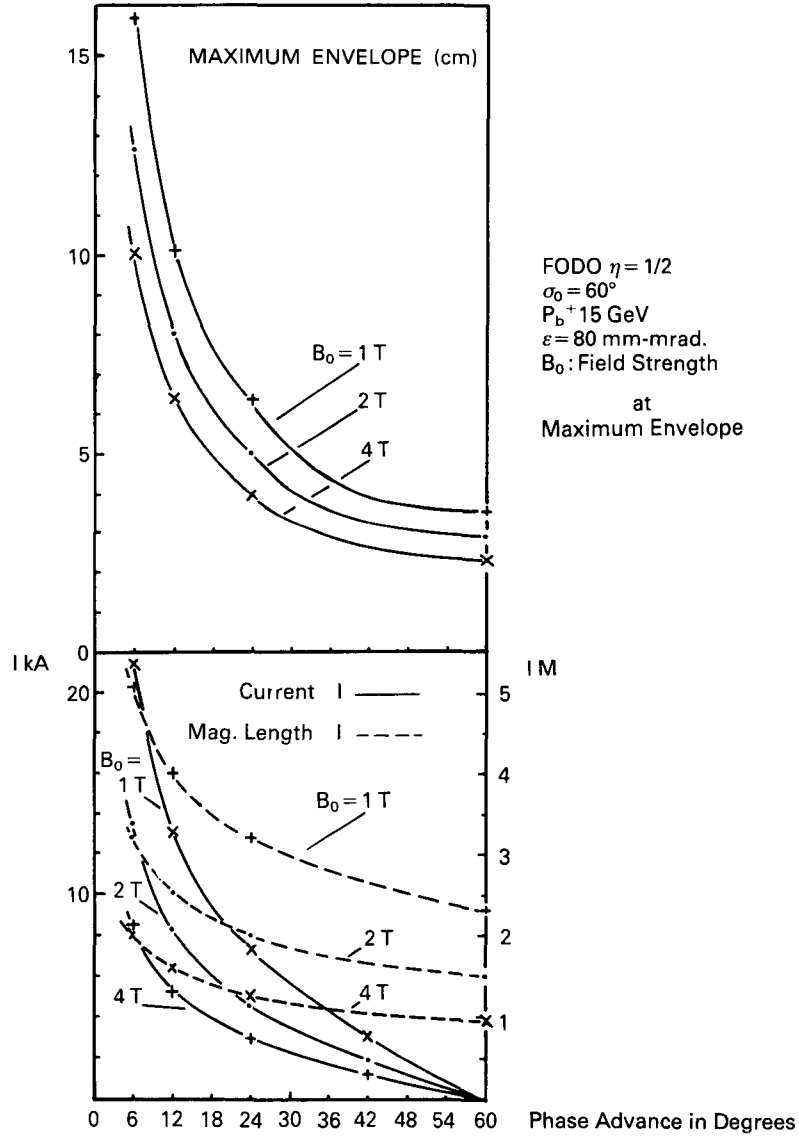


FIGURE 4. Scaling laws for periodic transport.

transport. The initial beam with longitudinal bunch length L_0 and momentum spread $(\Delta p/p)_0$ is presented as a phase space ellipse (figure 5). The initial tilt of the phase space ellipse is obtained by the ramped voltage of an induction linac of several hundred meters length. The phase rotation is performed in a drift section of about 1 kilometer length. During this drift, $\Delta p/p$ is reduced by a space charge repulsive force $(\Delta p/p)_f < (\Delta p/p)_i$. Longitudinal bunch compression is described by an envelope equation,

$$\frac{d^2 z_m}{ds^2} = -\frac{qeE_0\alpha}{Amc^2\gamma^3\beta^2} z_m + \frac{\epsilon^2}{\gamma^4 z_m^3} + \frac{3q^2}{2A} \frac{g}{\beta^2\gamma^5} \frac{Nr_i}{z_m^2} \quad (19)$$

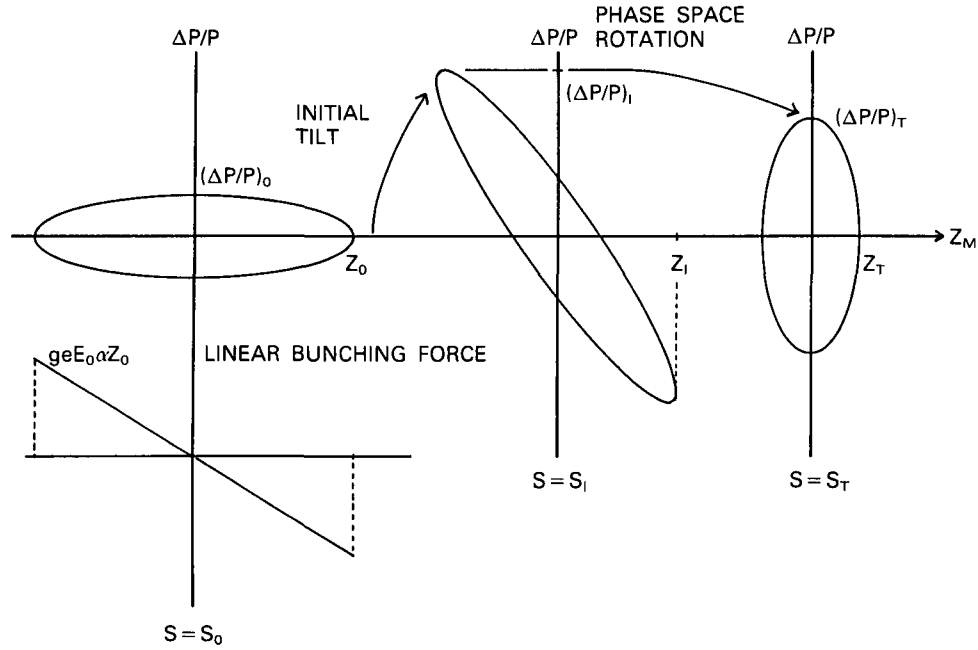


FIGURE 5. Bunch compression with linear induction voltage ramp and subsequent drift sections.

with:

- z_m = longitudinal envelope (bunch half-length) in z
- $\varepsilon = 1/\pi \times$ longitudinal emittance in $(z, \Delta p/p) = (\Delta p/p)/z_m$ for upright ellipse
- q = charge state
- A = mass number
- r_i = classical proton radius ($= 1.546 \times 10^{-18}$ m)
- N = total number of ions in bunch
- g = geometric factor $\sim 1 + 2 \ln R_{\text{wall}}/R_{\text{beam}}$
- $qeE_0\alpha z$ = linear bunching force of linac.

This equation assumes a linear space charge force, i.e. parabolic line density. Assuming constant longitudinal emittance during bunching, the momentum spread $(\Delta p/p)_i$ necessary to achieve the designed final beam half-length z_i and final momentum spread $(\Delta p/p)_f$ with ε , $(\Delta p/p)_i$ is,

$$\left(\frac{\Delta p}{p}\right)_f^2 = \left(\frac{\Delta p}{p}\right)_i^2 + 3 \frac{q^2}{A} \frac{g}{\beta^2 \gamma} \frac{N r_i}{z_i}. \quad (20)$$

The total voltage necessary to obtain this tilt of phase space ellipse with $(\Delta p/p)_i$ is given by,

$$qeE_0\alpha z_0 s \approx \frac{\gamma + 1}{\gamma} T \left(\frac{\Delta p}{p}\right)_i \quad [\text{coulomb} \cdot \text{volt}] \quad (21)$$

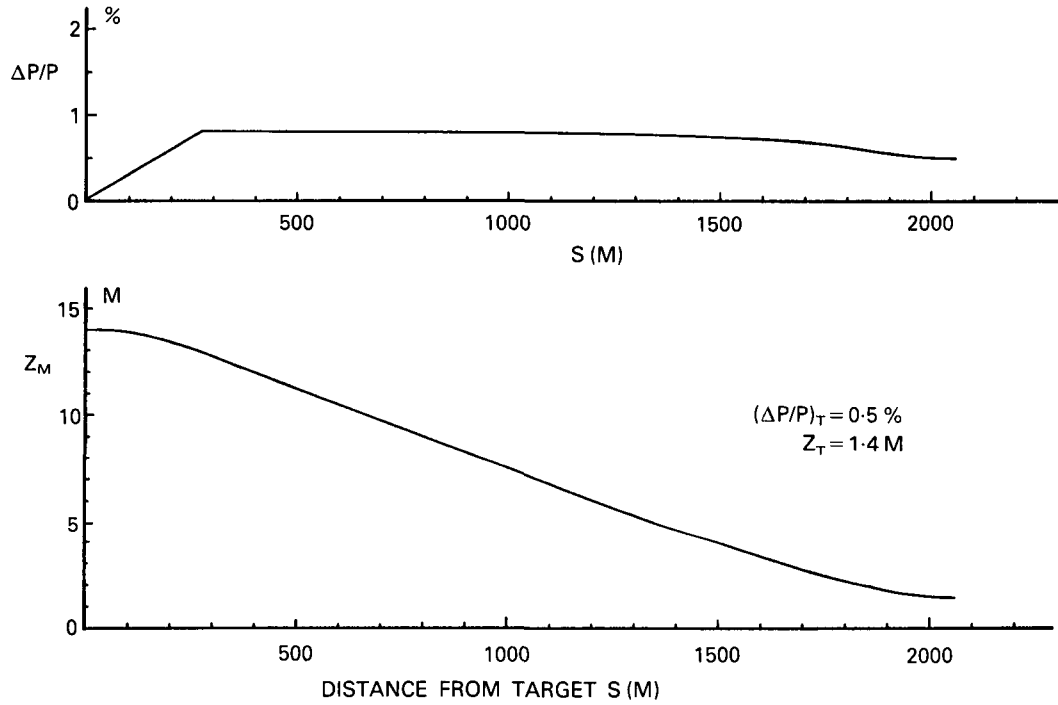


FIGURE 6. Longitudinal envelope solution.

where:

T = kinetic energy

s = length of the linac section.

$(\Delta p/p)_i$ is limited by chromatic aberration of the final focusing system. We take $(\Delta p/p)_i = 0.5 \sim 1.0\%$. In the real case, dilution of the emittance due to non parabolic shape and a finite $\Delta g/g$ -effect may occur.

Figure 6 shows the solution of the envelope equation for the example of ten-fold bunch compression. Total voltages $V/q = eE_0\alpha z_0 s$, necessary to tilt the ellipse are $V/q = 264$ MV for $(\Delta p/p)_i = 0.5 \times 10^{-2}$. We further assume that the bunching voltage $V/s = 1$ MV/m and $g = 2$. ($R_w/R_b = 1.65$). It is concluded that the total length of the final transport line from the buncher ring to the target is about 1.58 km in the case $(\Delta p/p)_i = 1\%$.

7.3. Final focusing on the target

The Kapchinskij-Vladimirskij envelope equation is solved to see the beam radius at the entry of the reactor chamber (5.5 m from the target) for different beam sizes at the target. Figure 7 shows the envelope solutions for the final current 1.78 kA of a 15 GeV Pb^+ beam with $\epsilon = 80$ mm mrad. It is concluded that the beam radius on entry is ~ 15 cm for a 3 mm radius spot at the target.

Focusing beams on the small target pellet requires some consideration of chromatic and geometrical aberrations. To keep the spot size diffusion on the target due to the

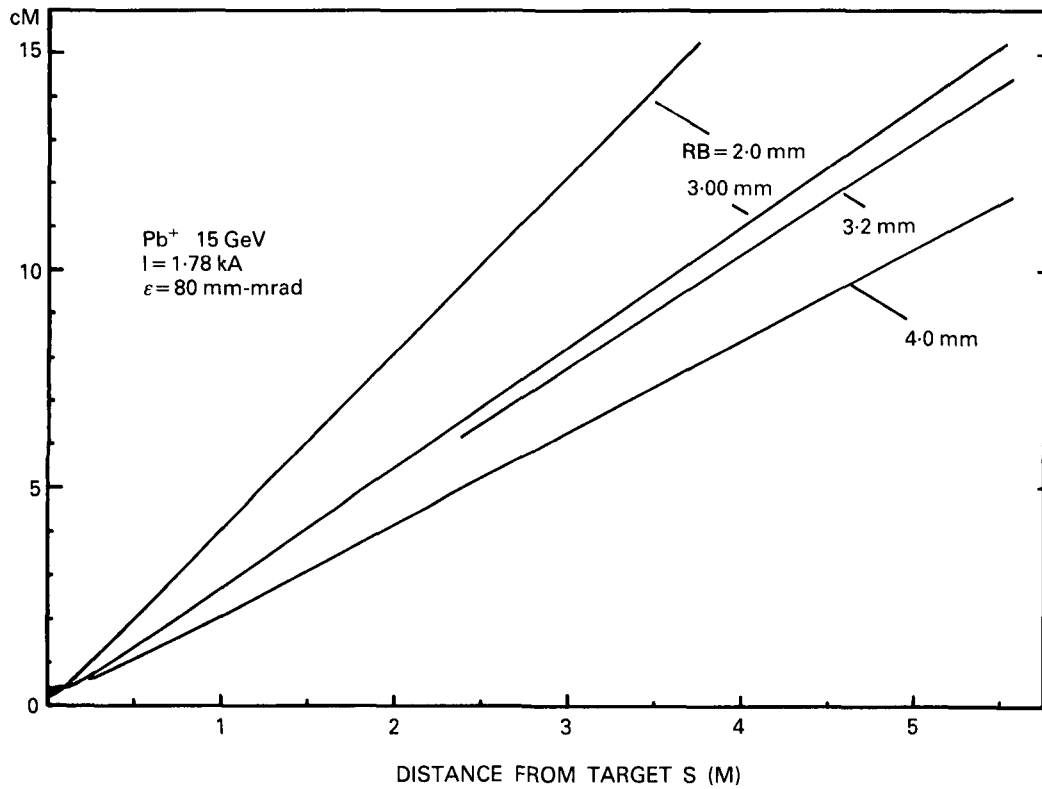


FIGURE 7. Envelope solutions in final focusing drift section for different beam sizes at target.

chromatic aberration below the target size, $\Delta p/p$ must satisfy the following condition,

$$\Delta p/p \leq \frac{r_t^2}{\epsilon L} \frac{1}{1 + \alpha}$$

where

r_t = target radius 4 mm

L = 5.5 m distance between target and final focusing element

α = 5 ~ 6.

α is related to the variation of the envelope and can be minimized by keeping the envelope as smooth as possible. Hence $\Delta p/p \leq 0.6\%$. To keep α small, steep waists in the envelope must be avoided. However, to protect the bending magnets and the quadrupole magnets in the transport and focusing system from the radiation coming from the reactor, we must put a waist in the envelope for shielding between the final quadrupole triplet and the upstream transport system. Figure 8 shows an example of an envelope solution with space charge between the target and the waist through the final quadrupole triplet. In this example, the spot size is also affected by geometric aberrations. Hence it is necessary to take into account the aberration correction with space charge in a more practical design of the focusing system.

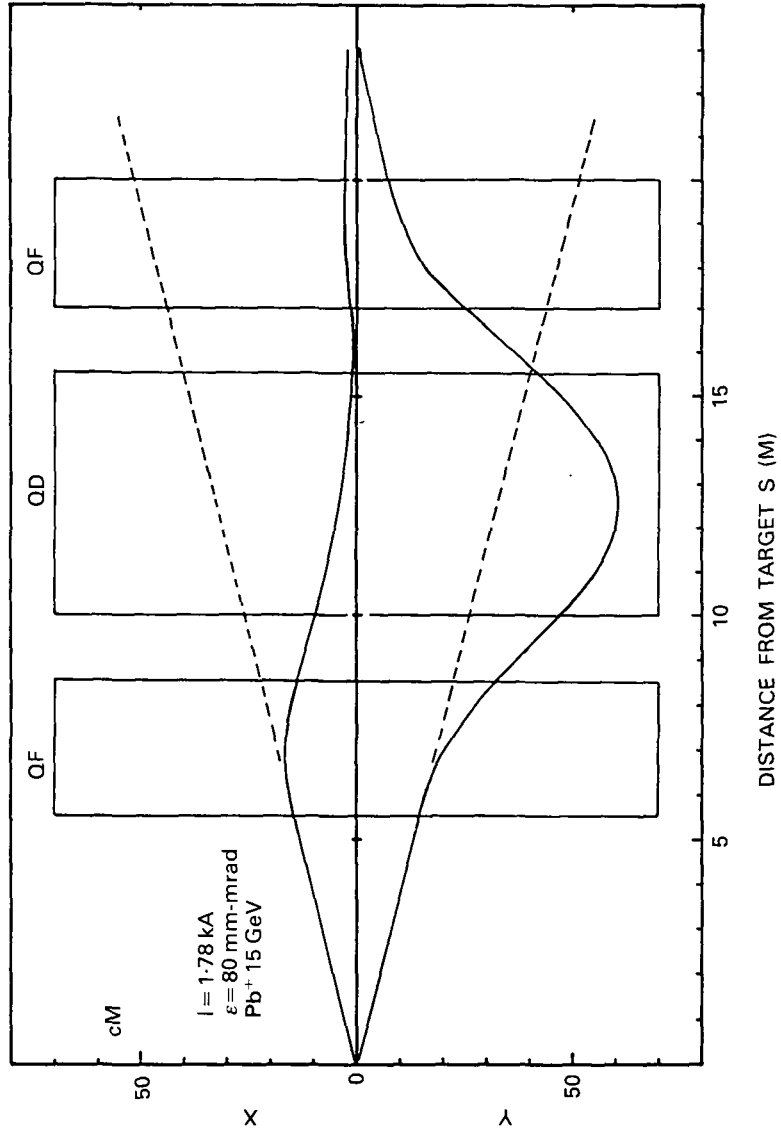


FIGURE 8. Envelope solutions with space charge in the final quadrupole triplet.

Acknowledgements

This work has been performed as a collaboration between the members of a working group for a heavy ion fusion driver system. A full report of the work is published as an internal report (Fujii-e *et al*, 1984) of the Institute of Plasma Physics, Nagoya University. It is a pleasure for the authors to give thanks to all the members of the working group. Drs. I. Hofmann and H. Eickhoff are acknowledged for their helpful discussions on the beam transport and multiturn injection simulations.

REFERENCES

- BOZSIK, I. & HOFMANN, I. 1981 *Nucl. Instr. Meth.* **187**, 305.
FUJII-E Y. *et al.* 1984 *Heavy Ion Fusion Reactor "HIBLIC-I"*, IPPJ-663.
HABER, I. 1979 *IEEE Trans. N.S.* **26**, 3090.
HABER, I. & MASCHKE, A. 1979 *Phys. Rev. Lett.* **42**, 1479.
KAPCHINSKIJ, I. M. & VLADIMIRSKIJ, V. V. 1959 *Proc. Int. Conf. on High Energy Acc., CERN*
KEIL, E. & SCHNELL, W. 1969 *CERN-ISR-TH-RF/69-48*.
LAPOSTOLLE, P. M. 1978 *CERN-ISR/78-13*
LASLETT, L. J. & SMITH, L. 1979 *IEEE Trans. N.S.* **26**, 3080.
MÖHL, D. 1979 *Proc. of HIF Workshop, Berkeley*.
NIU, K. 1984 *Contribution to the Conference on Heavy Ion Beam Fusion, Tokyo, Jan 1984*.
PENNER, S. & GALEJS, A. 1979 *IEEE Trans. N.S.* **26**, 3086.
SMITH, L. CHATTOPADHAY, S. HOFMANN, I. & LASLETT, L. J. 1977 *HIFAN 13-15*, LBL
ZOTTER, B. 1977 *CERN 77-13* 175.